

# SCIENTIFIC REPORTS



OPEN

## Spinal Hb9::Cre-derived excitatory interneurons contribute to rhythm generation in the mouse

Vanessa Caldeira<sup>1</sup>, Kimberly J. Dougherty<sup>1,2</sup>, Lotta Borgius<sup>1</sup> & Ole Kiehn<sup>1</sup>

Received: 25 July 2016

Accepted: 20 December 2016

Published: 27 January 2017

Rhythm generating neurons are thought to be ipsilaterally-projecting excitatory neurons in the thoracolumbar mammalian spinal cord. Recently, a subset of *Shox2* interneurons (*Shox2* non-V2a INs) was found to fulfill these criteria and make up a fraction of the rhythm-generating population. Here we use *Hb9::Cre* mice to genetically manipulate *Hb9::Cre*-derived excitatory interneurons (INs) in order to determine the role of these INs in rhythm generation. We demonstrate that this line captures a consistent population of spinal INs which is mixed with respect to neurotransmitter phenotype and progenitor domain, but does not overlap with the *Shox2* non-V2a population. We also show that *Hb9::Cre*-derived INs include the comparatively small medial population of INs which continues to express *Hb9* postnatally. When excitatory neurotransmission is selectively blocked by deleting *Vglut2* from *Hb9::Cre*-derived INs, there is no difference in left-right and/or flexor-extensor phasing between these cords and controls, suggesting that excitatory *Hb9::Cre*-derived INs do not affect pattern generation. In contrast, the frequencies of locomotor activity are significantly lower in cords from *Hb9::Cre-Vglut2<sup>Δ/Δ</sup>* mice than in cords from controls. Collectively, our findings indicate that excitatory *Hb9::Cre*-derived INs constitute a distinct population of neurons that participates in the rhythm generating kernel for spinal locomotion.

Locomotor behaviors, such as flying, swimming or walking, are complex motor actions that give animals and humans the ability to move and interact with the surroundings. The generation of locomotion in vertebrates is largely determined by neural networks in the spinal cord<sup>1–4</sup>. These spinal networks are responsible for key features that characterize limbed locomotion in mammals, rhythm generation and the precise coordination of muscle activation. In the ventral spinal cord where the locomotor circuit is located<sup>5</sup>, developmentally expressed transcription factors<sup>6,7</sup> have allowed for the identification and targeted manipulation of selected interneuron populations<sup>3,8–10</sup>. These studies have provided insights into the organization of the neuronal circuits underlying left-right<sup>11–16</sup> and flexor-extensor<sup>17–19</sup> coordination in mammals. Optogenetic, pharmacological, and lesion studies have provided strong evidence that the rhythmic drive in the mammalian spinal locomotor circuit comes from activity in ipsilaterally-projecting excitatory glutamatergic neurons<sup>1–3,9,20–24</sup>. However, despite the ablation of entire progenitor domain-derived classes of ipsilaterally-projecting excitatory neurons, rhythm-generating interneurons still remain elusive<sup>12,14,16,25–27</sup>. Therefore, there has also been focus on identifying and studying cell populations that span several progenitor domains. Recently, one such study directly linked rhythm generation to a group of excitatory interneurons identified by the embryonic expression of the transcription factor short stature homeobox protein 2 (*Shox2*)<sup>28</sup>. *Shox2* neurons span several of the dorsally and ventrally progenitor domain-derived interneuron classes, and partially overlap with V2a neurons which express the transcription factor *Chx10* during development<sup>28–30</sup>. *Shox2* non-V2a neurons were shown to be involved in rhythm generation<sup>28</sup>. However, eliminating *Shox2* non-V2a neurons from the network did not result in complete abolition of locomotor rhythm. Collectively, these data suggest that glutamatergic interneuron populations other than those captured in the current transcription factor schemas are involved in rhythm generation. To target such populations we are examining currently available genetic tools that may define unique neuronal groups to which we can ascribe such a function.

<sup>1</sup>Mammalian Locomotor Laboratory, Department of Neuroscience, Karolinska Institutet, 171 77 Stockholm, Sweden. <sup>2</sup>Department of Neurobiology and Anatomy, Drexel University College of Medicine, Philadelphia, PA 19129, US. Correspondence and requests for materials should be addressed to K.J.D. (email: kimberly.dougherty@drexelmed.edu) or O.K. (email: Ole.Kiehn@ki.se)

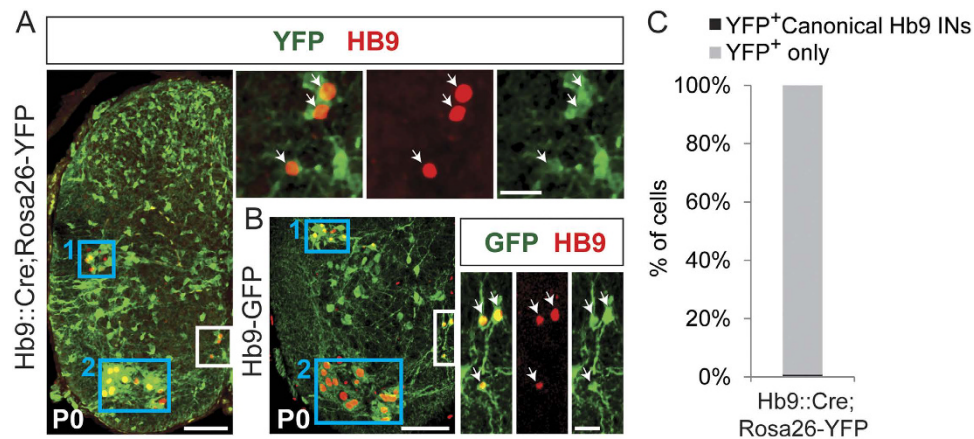


**Figure 1. Distribution of Hb9::Cre-derived INs and canonical Hb9 INs in the mouse rostral lumbar P0 spinal cord.** (A) Distribution of Hb9::Cre-derived INs (green), as marked by YFP expression (*Hb9::Cre;Rosa26-YFP* mice), and canonical Hb9 INs (white boxed area), as marked by HB9 protein expression (red) in medial lamina VIII. Preganglionic neurons (blue box 1) and motor neurons (blue box 2) also express HB9 protein in both *Hb9-GFP* and *Hb9::Cre; Rosa26-YFP* mice. Upper rightmost pictures are magnifications of the white boxed area containing canonical Hb9 INs. Arrowheads indicate overlap between Hb9::Cre-derived INs (YFP, green) and canonical Hb9 INs (Hb9 antibody, red). Scale bars: 100  $\mu$ m and 25  $\mu$ m. (B) Distribution of eGFP neurons (green) in the ventral spinal cord of *Hb9-GFP* mice, and the subset of canonical Hb9 INs (white boxed area), as marked by the overlap of HB9 protein (red) and GFP expression in medial lamina VIII. Rightmost pictures are magnifications of the white boxed area. Arrowheads indicate overlap between GFP (green) and HB9 protein (red). Scale bars: 100  $\mu$ m and 25  $\mu$ m. (C) Bar graph showing the percentage of the Hb9::Cre-derived IN population (represented by YFP expression, YFP<sup>+</sup>) that corresponds to canonical Hb9 INs (YFP<sup>+</sup> Canonical Hb9 INs) in *Hb9::Cre;Rosa26-YFP* mice. Canonical Hb9 INs account for less than 1% (0.86%  $\pm$  0.37%, darker grey) of the Hb9::Cre-derived IN population.

One group of interest is the group of neurons labeled by the transcription factor Hb9. Hb9 is usually described as a postmitotic motor neuron marker<sup>31</sup>, however, it is also transiently expressed in a larger group of progenitor cells and postmitotic neurons embryonically<sup>32</sup>. As it is commonly done when targeting spinal cord interneuron populations, we use conditional genetics and rely on Cre-dependent recombination to reliably target excitatory interneurons identified by the developmental expression of Hb9. This approach includes the small medial subset of interneurons retaining HB9 protein expression postnatally, which have been extensively studied and found to be excitatory neurons displaying cellular properties consistent with being potential rhythm generating neurons<sup>33–39</sup>.

In the current study, we selectively silence glutamatergic synaptic transmission in Hb9::Cre-derived excitatory neurons while retaining motor neuron output. We demonstrate that although reporter expression observed in *Hb9::Cre* mice represents a much larger population of neurons than those expressing the HB9 protein postnatally, the population identified is consistent and can be reliably used to target and manipulate a novel excitatory neuronal population in the spinal cord. We also show that excitatory Hb9::Cre-derived interneurons do not overlap with the *Shox2* non-V2a population. Synaptically silencing the excitatory subset of Hb9::Cre-derived interneurons by a targeted deletion of the vesicular glutamate transporter 2 (*Vglut2*) leads to a significant reduction in locomotor frequency without any significant effect in pattern formation, suggesting a role in rhythm generation. Taken together, our findings indicate that excitatory Hb9::Cre-derived interneurons constitute a second population of neurons, distinct from the *Shox2* non-V2a, which appear to be involved in the rhythm-generating kernel for mammalian locomotion.

## Results

**Hb9::Cre-derived INs are located in the ventral and dorsal spinal cord.** Although *Hb9::Cre*<sup>40</sup> and *Hb9-GFP*<sup>41</sup> mice were generated with an analogous strategy to the *Hb9-LacZ* mice<sup>31</sup>, reporter expression in *Hb9::Cre-reporter-labeled* (*Hb9::Cre;Rosa26-FP*) and *Hb9-GFP* mice is not restricted to motor neurons (MNs). In the *Hb9-GFP* mouse, a ventral population of interneurons is marked<sup>41</sup>, whereas in the *Hb9::Cre;Rosa26-FP* mouse line a dorsal population of cells is also captured. The increase in the number and laminar distribution of fluorescent reporter cells observed in *Hb9::Cre;Rosa26-FP* mice may be attributed to the transient embryonic expression of Hb9 in these cells<sup>32,42</sup>.

YFP expression in *Hb9::Cre;Rosa26-YFP* mice was detected through lamina I to VI in addition to lamina VII, VIII and ventral X (Fig. 1A) throughout the lumbar spinal cord. This is in contrast to the GFP expression in *Hb9-GFP* mice<sup>33</sup>, which is restricted to lamina VII, VIII and ventral X (Fig. 1B). We will collectively refer to these dorsal (lamina I–VI) and ventral neuronal populations in *Hb9::Cre;Rosa26-FP* mice as Hb9::Cre-derived INs.

Despite the larger number of reporter-expressing cells in *Hb9::Cre;Rosa26-FP* mice, reporter expression identifies a consistent group of interneurons throughout the lumbar spinal cord. Thus, we use the *Hb9::Cre* mouse as a genetic tool to study the possible roles of excitatory Hb9::Cre-derived INs in locomotion.

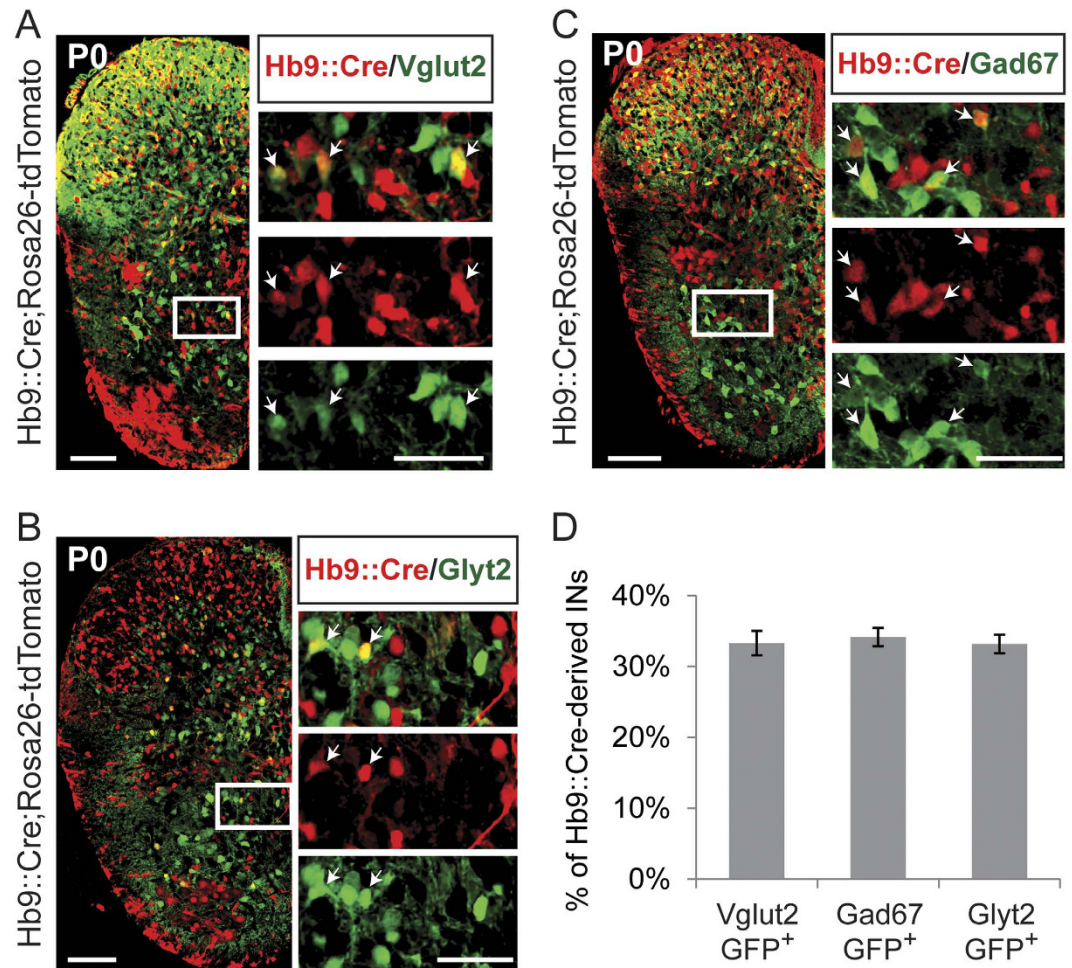


**Figure 2. One third of the Hb9::Cre-derived INs are excitatory.** (A,B and C) Transverse spinal cord hemisections, at segmental levels L1-L3 of P0 mice, showing co-expression of tdTomato fluorescent protein (red) (*Hb9::Cre;Rosa26-tdTomato* mice) with GFP (green) from *Vglut2-GFP* (A), *Glyt2-GFP* (B), and *Gad67-GFP* (C) mice. Rightmost pictures are magnifications of the white boxed areas. Arrowheads indicate overlap between Hb9::Cre-derived INs (tdTomato protein, red) and Vglut2, Glyt2, or Gad67-GFP neurons (GFP protein, green). Scale bars represent 100  $\mu$ m for the transverse hemi-sections and 50  $\mu$ m for the magnified boxes on the right. (D) Percent of Hb9::Cre-derived INs that are glutamatergic (Vglut2-GFP<sup>+</sup>, 33%  $\pm$  2%), GABAergic (Gad67-GFP<sup>+</sup>, 34%  $\pm$  1%), and glycinergic (Glyt2-GFP<sup>+</sup>, 33%  $\pm$  1%) in Hb9::Cre;Rosa26-tdTomato spinal cords.

**Canonical Hb9 INs account for less than 1% of the Hb9::Cre-derived IN population.** We first asked if the Hb9::Cre-derived INs include the canonical Hb9 INs. We define canonical Hb9 INs as the small subset of neurons clustered in medial lamina VIII in the lower thoracic and upper lumbar mouse spinal cord. These interneurons retain endogenous HB9 protein expression postnatally and also co-express GFP protein under the Hb9 promoter in *Hb9-GFP* mice (type I cells referred in refs 33 and 35) (Fig. 1B, white boxed area). These canonical Hb9 neurons have been suggested to be part of the kernel for rhythm generation in the mammalian locomotor network<sup>33–36</sup>.

In *Hb9::Cre;Rosa26-YFP* mice, an overlap of YFP and HB9 protein was evident in canonical Hb9 INs, motor neurons (MNs) and sympathetic preganglionic neurons (Fig. 1A). We indeed found that the majority of canonical Hb9 INs co-express HB9 protein and the reporter protein, YFP, in *Hb9::Cre;Rosa26-YFP* mice (86%  $\pm$  7%, N = 3, 18 sections). Conversely, canonical Hb9 INs make up less than 1% (0.86%  $\pm$  0.37%) of the Hb9::Cre-derived IN population (N = 3, 18 sections) (Fig. 1C). The number of canonical Hb9 neurons (193  $\pm$  61 cells between Th12 and L3, N = 3) is similar to what was previously reported<sup>33</sup>. Taken together these data indicate that most of the canonical Hb9 INs are part of Hb9::Cre-derived IN population, but they account for a very small percentage of this population. Therefore, hereinafter whenever we refer to the Hb9::Cre-derived INs, the canonical Hb9 INs in Th12-L3 will be implicitly included.

**One third of Hb9::Cre-derived INs are glutamatergic.** We next sought to assess the transmitter phenotype of the Hb9::Cre-derived IN population by examining overlap of reporter expression in *Hb9::Cre;Rosa26-tdTomato;Vglut2-GFP*, *Hb9::Cre;Rosa26-tdTomato;Glyt2-GFP*, and *Hb9::Cre;Rosa26-tdTomato;Gad67-GFP*

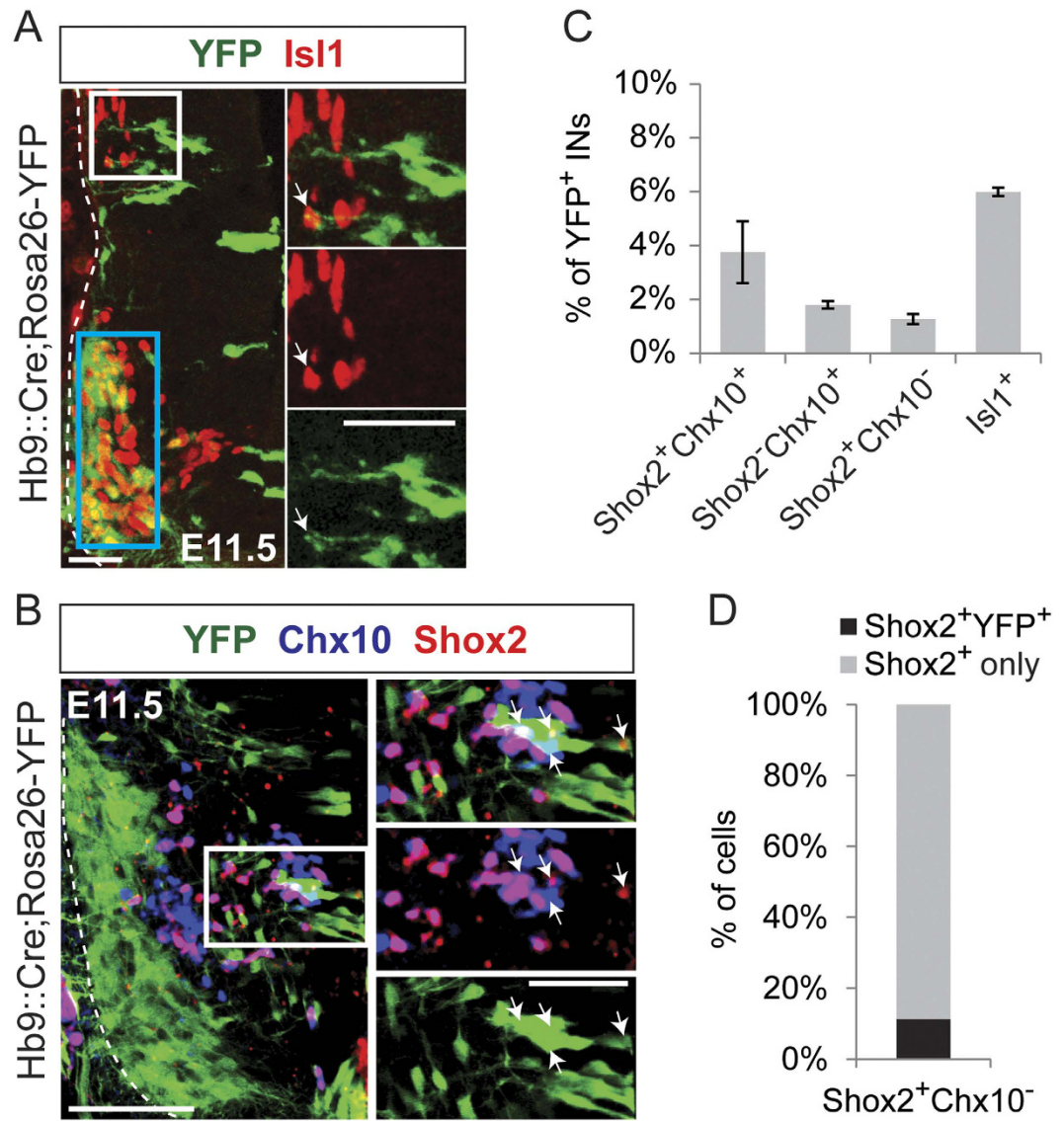


**Figure 3. Hb9::Cre-derived INs do not overlap with the Shox2 non-V2a population.** (A) Co-expression of YFP (green) and Isl1 antibody (red) in the *Hb9::Cre; Rosa26-YFP* mouse spinal cord at E11.5. Motor neurons are also labeled by Isl1 antibody (blue box). Rightmost pictures are magnifications of the white boxed area. Arrowheads indicate overlap between Isl1 (red) and Hb9::Cre-derived INs (green). Scale bars: 100  $\mu$ m and 50  $\mu$ m. (B) Co-expression of YFP (green), Shox2 antibody (red) and/or Chx10 antibody (blue) in the *Hb9::Cre; Rosa26-YFP* mouse ventral spinal cord at E11.5. Rightmost pictures are magnifications of the white boxed area. Arrowheads indicate overlap between Hb9::Cre-derived INs (green) and Shox2<sup>+</sup> Chx10<sup>+</sup> (red), Shox2<sup>-</sup> Chx10<sup>+</sup> (blue) or Shox2<sup>+</sup> Chx10<sup>-</sup> (pink). Scale bars: 100  $\mu$ m and 50  $\mu$ m. (C) Quantification of overlap in (A) and (B). Bar graph showing percent of overlap between Hb9::Cre-derived INs (YFP<sup>+</sup>) and Shox2 V2a (Shox2<sup>+</sup> Chx10<sup>+</sup>, 4%  $\pm$  1%), Shox2<sup>OFF</sup> V2a (Shox2<sup>-</sup> Chx10<sup>+</sup>, 2%  $\pm$  0.1%), Shox2 non-V2a (Shox2<sup>+</sup> Chx10<sup>-</sup>, 1.3%  $\pm$  0.2%), and Isl1 (Isl1<sup>+</sup>, 6%  $\pm$  0.2%) INs. Error bars represent  $\pm$  SEM. (D) Percent of the Shox2 non-V2a IN population (Shox2<sup>+</sup> Chx10<sup>-</sup>) that overlaps with Hb9::Cre-derived INs (YFP<sup>+</sup>) in the *Hb9::Cre; Rosa26-YFP* mouse spinal cord at E11.5. Shox2 non-V2a INs rarely co-express YFP (Shox2<sup>+</sup> YFP<sup>+</sup>, darker grey) (12%  $\pm$  2%). Error bars represent  $\pm$  SEM.

mice, in order to identify Hb9::Cre-derived glutamatergic (Fig. 2A), glycinergic (Fig. 2B), and GABAergic (Fig. 2C) neurons, respectively. Motor neurons were easily recognized by size and location and were excluded from all counts. The transmitter phenotype of Hb9::Cre-derived INs is mixed; approximately 1/3 are excitatory (33%  $\pm$  2% Vglut2) and 2/3 are inhibitory (34%  $\pm$  1% GAD67, and 33%  $\pm$  1% GlyT2) (N = 3 animals per condition, 48 sections) (Fig. 2D).

**Hb9::Cre-derived INs span several progenitor domains, but constitute a population distinct from the Shox2-nonV2a INs.** To further characterize the excitatory Hb9::Cre-derived IN population, we turned to the developmentally expressed transcription factors found in excitatory neurons, and looked for overlap

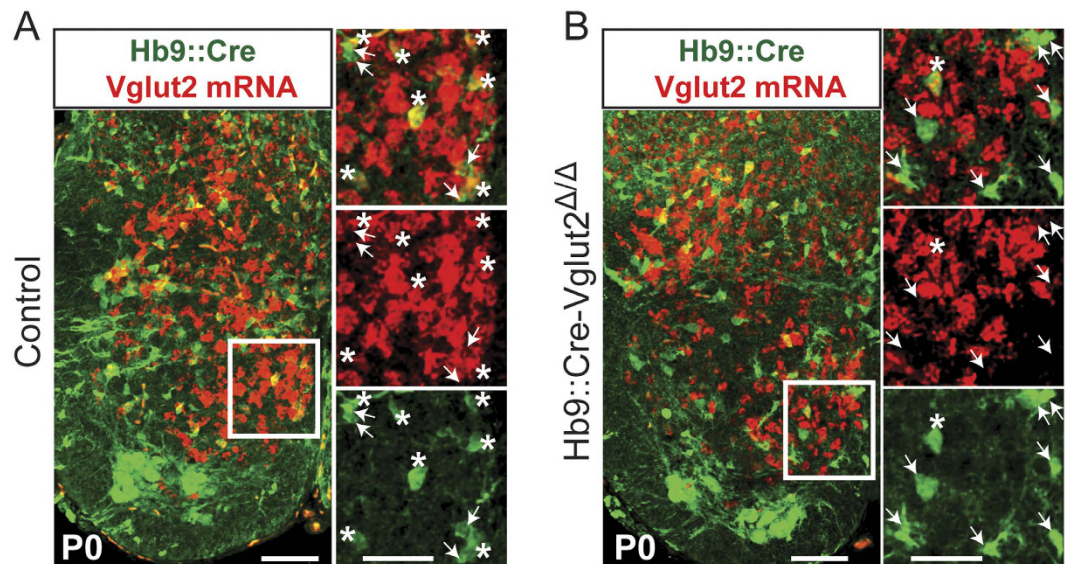


**Figure 4.** Loss of *Vglut2* expression in *Hb9::Cre-Vglut2 $\Delta/\Delta$*  mice. (A and B) Fluorescent *in situ* hybridization shows co-localization of *Vglut2* mRNA (red) and *Hb9::Cre*-derived INs (YFP, green) in control (*Hb9::Cre; Vglut2<sup>Fllox/+</sup>; Rosa26-YFP*) (A), and *Hb9::Cre-Vglut2 $\Delta/\Delta$*  (*Hb9::Cre; Vglut2 $\Delta/Fllox$ ; Rosa26-YFP*) (B) P0 spinal cords. Rightmost pictures are magnifications of the white boxed areas. Asterisks indicate *Vglut2* mRNA detected in *Hb9::Cre*-derived INs. Arrowheads indicate the absence of *Vglut2* mRNA in *Hb9::Cre*-derived INs. Scale bars represent 100  $\mu$ m for the transverse hemi-sections and 50  $\mu$ m for the magnified boxes on the right.

with the exclusively excitatory and ipsilateral IN markers, *Isl1*, *Chx10* and *Shox2* (Fig. 3A and B respectively). All experiments were performed at embryonic stage E11.5 to capture the peak of expression of these early neuronal markers.

The LIM homeodomain transcription factor 1 (*Isl1*) is expressed in MNs and is involved in MN differentiation<sup>31</sup>. Its expression defines a class of interneurons, the dI3 INs<sup>43,44</sup>, which have been shown to be involved in the cutaneous regulation of paw grasp<sup>26</sup> but not in locomotor rhythm or patterning. Therefore, we sought to investigate whether or not dI3 INs and *Hb9::Cre*-derived INs were overlapping. We found that *Hb9::Cre*-derived INs seldomly co-expressed *Isl1* ( $6\% \pm 0.2\%$ ,  $N = 2$ , 22 sections) (Fig. 3C), indicating that the dI3 IN population shows no appreciable overlap with the *Hb9::Cre*-derived INs.

*Chx10* is the marker for V2a neurons and the expression of *Shox2* and *Chx10* can be used to categorize excitatory neurons in the ventral spinal cord into three groups: *Shox2* V2a INs ( $Shox2^+ Chx10^+$ ), *Shox2* non-V2a INs ( $Shox2^+ Chx10^-$ ), and *Shox2<sup>OFF</sup>* V2a INs ( $Shox2^- Chx10^+$ )<sup>28</sup>. *Shox2* non-V2a INs is the only subgroup of excitatory neurons that has been shown to contribute to rhythm generation in mammals, whereas *Shox2* V2a INs, and *Shox2<sup>OFF</sup>* V2a INs seem to be involved in pattern generation<sup>28</sup>. We found that *Hb9::Cre*-derived INs rarely overlapped with the *Shox2* V2a ( $4\% \pm 0.1\%$ ), *Shox2<sup>OFF</sup>* V2a ( $2\% \pm 0.1\%$ ) and *Shox2* non-V2a ( $1.3\% \pm 0.2\%$ ) populations ( $N = 2$ , 22 sections) (Fig. 3C). Moreover, we also verified that *Hb9::Cre*-derived INs make up less than  $12\% \pm 2\%$  of the *Shox2* non-V2a population (Fig. 3D).

Altogether, these data indicate that although excitatory *Hb9::Cre*-derived INs are a heterogeneous group of neurons that span several excitatory progenitor domains, they make up a distinct group of excitatory neurons that only marginally overlaps with the *Shox2* non-V2a population.

#### **Vglut2 is effectively removed from excitatory *Hb9::Cre*-derived INs in *Hb9::Cre-Vglut2 $\Delta/\Delta$* mice.**

In order to selectively target excitatory *Hb9::Cre*-derived INs and investigate their role in locomotor network activity, *Hb9::Cre* mice were crossed with mice carrying a conditional floxed *Vglut2* allele to produce offspring with a Cre-dependent selective loss of *Vglut2* (see Experimental Procedures), thereby disrupting synaptic transmission exclusively in excitatory *Hb9::Cre*-derived INs. As shown in previous work from our lab and others, removal of *Vglut2* efficiently blocks action potential mediated synaptic transmission from the affected neurons<sup>17,26,28</sup>, and hence results in the functional removal of these neurons from the network.

To assess the loss of *Vglut2* transcript, we performed *in situ* hybridization with a *Vglut2* probe on spinal cord tissue from both mice which have complete removal of *Vglut2* from *Hb9::Cre*-derived neurons (*Hb9::Cre; Vglut2 $\Delta/Fllox$ ; Rosa26-YFP*, referred to as *Hb9::Cre-Vglut2 $\Delta/\Delta$* ) and littermates which have one copy of *Vglut2* removed but retain normal synaptic function (*Hb9::Cre; Vglut2<sup>Fllox/+</sup>; Rosa26-YFP*, referred to as controls). *Vglut2* signal was seen extensively throughout the gray matter in cords from both control (Fig. 4A) and *Hb9::Cre-Vglut2 $\Delta/\Delta$*  mice (Fig. 4B). However, *Vglut2* mRNA expression was reduced by 81% ( $N = 3$  animals per condition, 26 sections), in *Hb9::Cre*-derived INs, in *Hb9::Cre-Vglut2 $\Delta/\Delta$*  ventral spinal cords compared to controls.

#### **Silencing the synaptic signaling of excitatory *Hb9::Cre*-derived INs reduces the frequency of locomotor-like activity.**

To determine the functional impact of the loss of excitatory synaptic transmission

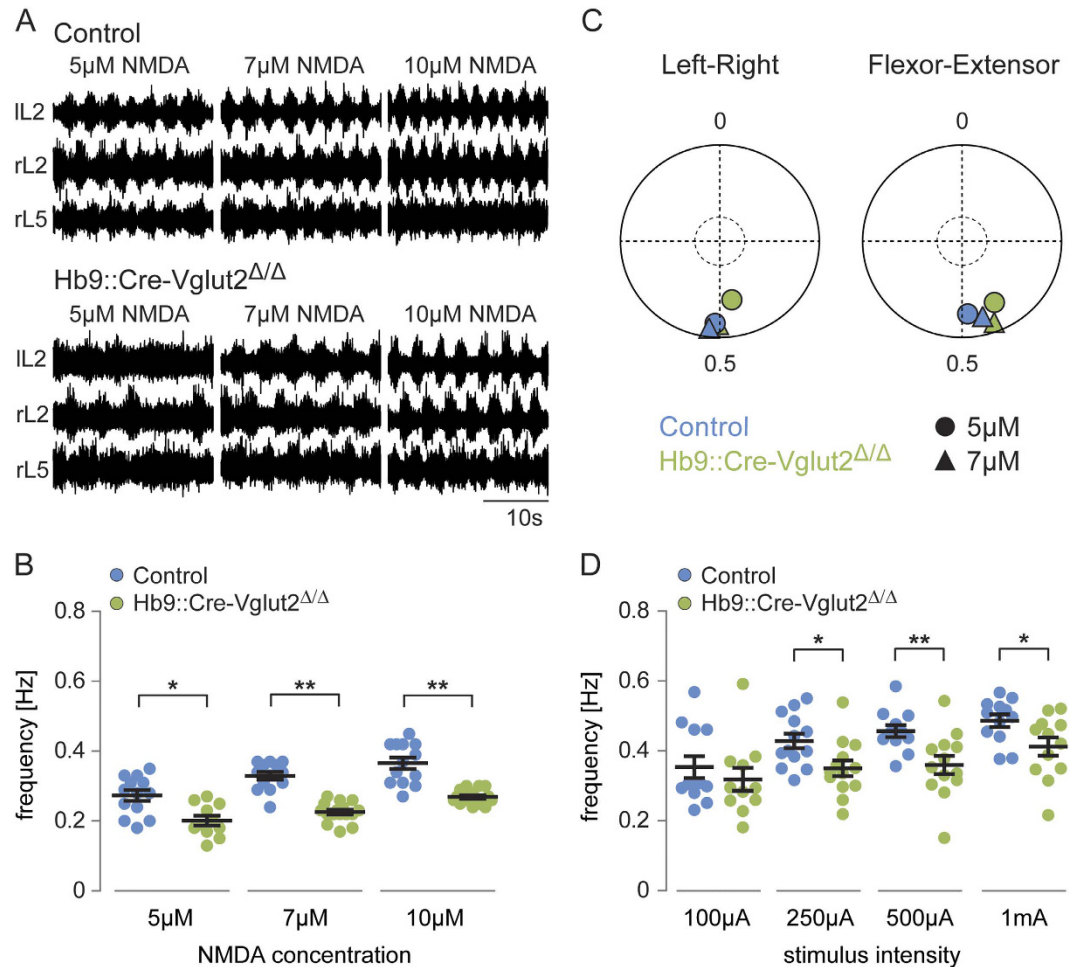


**Figure 5. Silencing the output of glutamatergic Hb9::Cre-derived INs leads to reduced frequency of drug-evoked and neural-evoked locomotor-like activity.** (A) Ventral root recordings of drug-evoked locomotor-like activity in control (upper traces) and Hb9::Cre-Vglut2 $\Delta/\Delta$  (lower traces) spinal cords at three concentrations of NMDA. All include 5-HT (8  $\mu$ M). (B) Frequency of locomotor-like activity as a function of NMDA concentration on a constant background of 5-HT (8  $\mu$ M) in control (blue) and Hb9::Cre-Vglut2 $\Delta/\Delta$  (green) spinal cords. Locomotor frequencies obtained in Hb9::Cre-Vglut2 $\Delta/\Delta$  cords were always lower than in control cords at all NMDA concentrations. Error bars represent  $\pm$  SEM. \*Indicates  $p < 0.001$  and \*\* indicates  $p < 0.0001$ . (C) Circular plots of mean left-right (IL2-rL2) and flexor-extensor (rL2-rL5) coordination in control (blue) and Hb9::Cre-Vglut2 $\Delta/\Delta$  (green) spinal cords at 5 and 7  $\mu$ M NMDA and 8  $\mu$ M 5-HT. Each point corresponds to the mean vector value for each drug concentration (Left-right controls: 5  $\mu$ M and 7  $\mu$ M NMDA (N = 11); Flexor-extensor controls: 5  $\mu$ M and 7  $\mu$ M NMDA (N = 10); Left-right Hb9::Cre-Vglut2 $\Delta/\Delta$  cords: 5  $\mu$ M NMDA (N = 8) and 7  $\mu$ M NMDA (N = 12)). Individual vector values were generated from 50 locomotor cycles in each spinal cord. The inner circle indicates significance level of  $p = 0.05$ . (D) Frequency of the descending fiber-evoked locomotor-like activity as function of stimulation amplitude. The maximal frequency obtained in Hb9::Cre-Vglut2 $\Delta/\Delta$  cords (green) was lower than in controls (blue) at stimulation strengths of 250  $\mu$ A – 1 mA (controls:  $0.35 \pm 0.03$  Hz (N = 12/13),  $0.43 \pm 0.02$  Hz (N = 13/13),  $0.46 \pm 0.02$  Hz (N = 12/13),  $0.49 \pm 0.02$  Hz (N = 12/13); Hb9::Cre-Vglut2 $\Delta/\Delta$  cords:  $0.32 \pm 0.03$  Hz (N = 11/16),  $0.35 \pm 0.02$  Hz (N = 13/16),  $0.36 \pm 0.03$  Hz (N = 13/16),  $0.41 \pm 0.03$  Hz (N = 12/16) at 100  $\mu$ A, 250  $\mu$ A, 500  $\mu$ A, and 1 mA, respectively). Error bars represent  $\pm$  SEM. \*Indicates  $p < 0.05$  and \*\*Indicates  $p < 0.005$ .

in Hb9::Cre-derived INs, we performed locomotor experiments in spinal cords isolated from early postnatal animals. Although Hb9::Cre-Vglut2 $\Delta/\Delta$  mice appear to breathe and have spontaneous movements, they do not survive to P1. Therefore, all experiments were performed at P0. Locomotor-like activity was evoked by bath application of NMDA and serotonin (5-HT). The concentration of 5-HT was kept at 8  $\mu$ M, while the NMDA was varied (5  $\mu$ M, 7  $\mu$ M, and 10  $\mu$ M) in order to test a range of locomotor frequencies. Locomotor-like activity was evoked in all controls (N = 13/13) (Fig. 5A, upper traces) and Hb9::Cre-Vglut2 $\Delta/\Delta$  cords (5  $\mu$ M, N = 11/16; 7  $\mu$ M and 10  $\mu$ M NMDA, N = 16/16) (Fig. 5A, lower traces). However, locomotor frequencies in Hb9::Cre-Vglut2 $\Delta/\Delta$  cords were 26–31% lower than that of controls at all NMDA concentrations tested ( $p < 0.0001$ ) (controls:  $0.27 \pm 0.02$  Hz at 5  $\mu$ M,  $0.33 \pm 0.01$  Hz at 7  $\mu$ M,  $0.36 \pm 0.02$  Hz at 10  $\mu$ M; Hb9::Cre-Vglut2 $\Delta/\Delta$  cords:  $0.20 \pm 0.01$  Hz

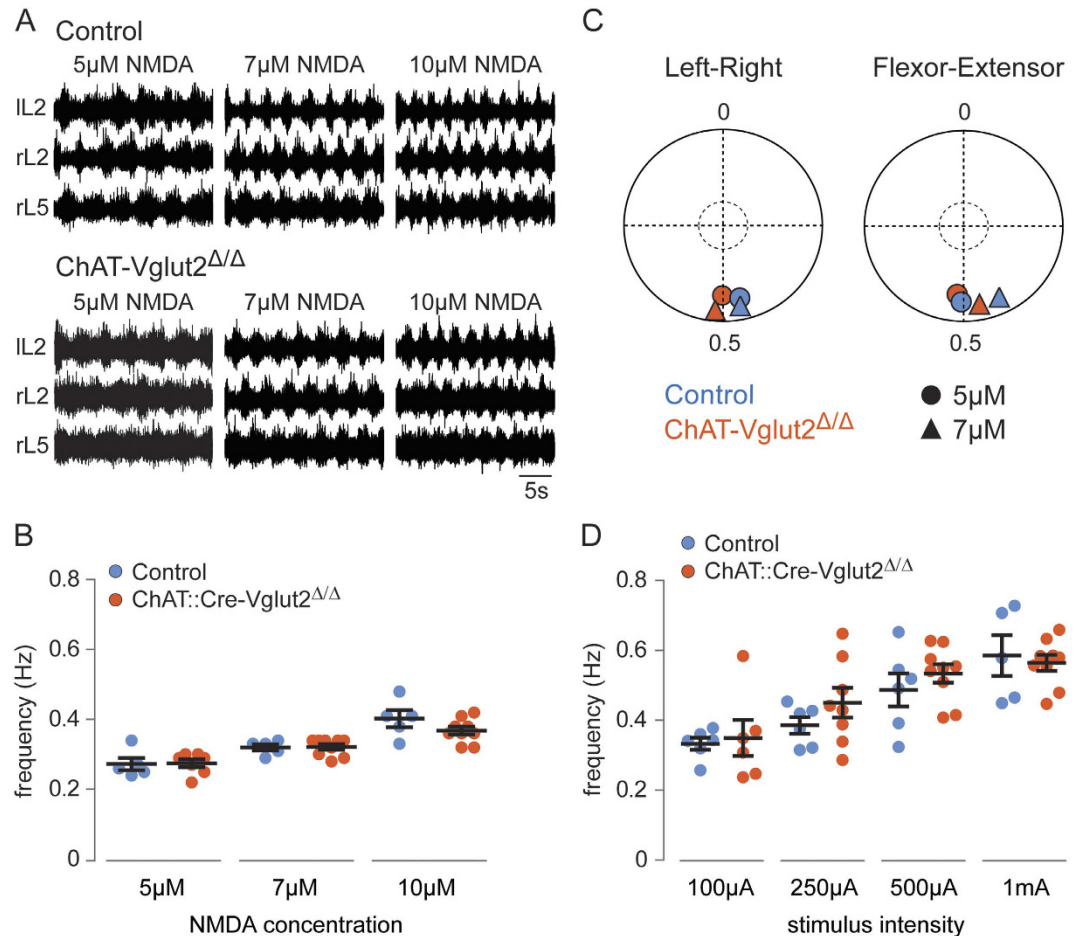


**Figure 6. Disruption of glutamatergic synaptic transmission in motor neurons does not affect locomotor frequency.** (A) Ventral-root recordings showing drug-induced rhythmic locomotor-like activity in control (upper traces) and ChAT-Vglut2 $\Delta/\Delta$  (lower traces) spinal cords at three concentrations of NMDA. All include 5-HT (8  $\mu$ M). (B) Frequency of locomotor-like activity induced by increasing concentrations of NMDA on a constant background of 5-HT (8  $\mu$ M) in control (blue) and ChAT-Vglut2 $\Delta/\Delta$  (red) spinal cords. Locomotor frequencies obtained in ChAT-Vglut2 $\Delta/\Delta$  cords were similar to that of control cords at all NMDA concentrations. Error bars represent  $\pm$  SEM. (C) Circular plots showing left-right (LL2-rL2) and flexor-extensor (rL2-rL5) phasing in control (blue) and ChAT-Vglut2 $\Delta/\Delta$  (red) spinal cords in different concentrations of NMDA and 8  $\mu$ M 5-HT. Each point corresponds to the mean vector value of all cords (Left-right controls: 5  $\mu$ M and 7  $\mu$ M NMDA (N = 6); Flexor-extensor controls: 5  $\mu$ M and 7  $\mu$ M NMDA (N = 4); Left-right ChAT-Vglut2 $\Delta/\Delta$  cords: 5  $\mu$ M NMDA (N = 8) and 7  $\mu$ M NMDA (N = 9); Flexor-extensor ChAT-Vglut2 $\Delta/\Delta$  cords: 5  $\mu$ M NMDA (N = 8) and 7  $\mu$ M NMDA (N = 9)) for each drug concentration. The inner circle indicates significance level of  $p = 0.05$ . (D) Frequency of descending fiber-evoked locomotor-like activity as a function of stimulation intensity in controls (blue) and in ChAT-Vglut2 $\Delta/\Delta$  cords (red). Locomotor frequencies obtained in ChAT-Vglut2 $\Delta/\Delta$  cords were similar to that of control cords at all stimulation intensities tested (controls:  $0.33 \pm 0.02$  Hz (N = 6/6),  $0.39 \pm 0.02$  Hz (N = 6/6),  $0.49 \pm 0.05$  Hz (N = 6/6),  $0.59 \pm 0.06$  Hz (N = 5/6); ChAT-Vglut2 $\Delta/\Delta$  cords:  $0.35 \pm 0.05$  Hz (N = 6/9),  $0.45 \pm 0.04$  Hz (N = 8/9),  $0.53 \pm 0.03$  Hz (N = 9/9),  $0.56 \pm 0.02$  Hz (N = 9/9) at 100  $\mu$ A, 250  $\mu$ A, 500  $\mu$ A, and 1 mA, respectively). Error bars represent  $\pm$  SEM.

at 5  $\mu$ M;  $0.23 \pm 0.006$  Hz at 7  $\mu$ M,  $0.27 \pm 0.005$  Hz at 10  $\mu$ M) (Fig. 5B). There was no significant difference in pattern generation as assessed by coordination of activity between the left and right sides of the cord (out of phase activity between right L2 and left L2) and in ipsilateral flexor-extensor coordination (out of phase activity between right L2 (flexor) and right L5 (extensor)) between control and Hb9::Cre-Vglut2 $\Delta/\Delta$  cords (Watson-William's Test,  $p > 0.09$ ). Mean left-right phase values (Fig. 5C, left) in controls were 0.51 (N = 11) and 0.52 (N = 11) at 5  $\mu$ M and 7  $\mu$ M NMDA, respectively, and in Hb9::Cre-Vglut2 $\Delta/\Delta$  cords were 0.47 (5  $\mu$ M NMDA, N = 8) and 0.50 (7  $\mu$ M NMDA, N = 13). Mean flexor-extensor phase values (Fig. 5C, right) in controls were 0.49 (5  $\mu$ M NMDA, N = 10) and 0.46 (7  $\mu$ M NMDA, N = 10) and in Hb9::Cre-Vglut2 $\Delta/\Delta$  cords were 0.41 (5  $\mu$ M NMDA, N = 8) and 0.44 (7  $\mu$ M NMDA, N = 12). Thus, left-right and flexor-extensor bursts were out of phase and close to alternation in both controls and Hb9::Cre-Vglut2 $\Delta/\Delta$  cords.

In addition to drug-evoked locomotion, we also tested the effects of the loss of excitatory Hb9::Cre-derived INs on locomotion evoked by neural stimulation. It was possible to evoke locomotor-like activity by stimulating

fibers descending from the brainstem in all control cords tested and in ~80% of the *Hb9::Cre-Vglut2 $\Delta/\Delta$*  cords (N = 13/16). The bursting frequency was reduced in *Hb9::Cre-Vglut2 $\Delta/\Delta$*  cords by 15–21% compared to controls at stimulation strengths of 250  $\mu$ A – 1 mA ( $p < 0.02$ ) (Fig. 5D). Additionally, during electrical stimulation, the bursting was more difficult to discriminate in spinal cords from *Hb9::Cre-Vglut2 $\Delta/\Delta$*  mice.

Together, the lower drug-evoked and stimulus-evoked locomotor frequencies seen in spinal cords from *Hb9::Cre-Vglut2 $\Delta/\Delta$*  mice compared to controls suggest that excitatory spinal *Hb9::Cre*-derived INs play a significant role in rhythm generation.

**Loss of glutamatergic synaptic transmission in motor neurons does not affect the frequency of drug-induced or neural-evoked locomotor activity.** *Hb9* is expressed by motor neurons<sup>31</sup> and mammalian motor neurons co-release glutamate and acetylcholine from central collaterals<sup>17,45,46</sup>. Since locomotion can be initiated by ventral root stimulation<sup>46,47</sup>, we sought to determine if loss of Vglut2-mediated glutamatergic synaptic transmission in motor neurons would contribute to the locomotor phenotype observed in *Hb9::Cre-Vglut2 $\Delta/\Delta$*  spinal cords.

Similarly to our approach with *Hb9::Cre* mice, *ChAT::Cre* mice were used to generate *ChAT-Vglut2 $\Delta/\Delta$*  mice in which glutamatergic synaptic transmission was selectively lost in cholinergic neurons, including MNs. *ChAT-Vglut2 $\Delta/\Delta$*  mice are viable and show no clear phenotype; however, all experiments were performed at P0 for consistency. Locomotor-like activity was induced by bath application of NMDA (5  $\mu$ M–10  $\mu$ M) and 5-HT (8  $\mu$ M), and it was evoked in all control (N = 5/5) (Fig. 6A, upper traces) and *ChAT-Vglut2 $\Delta/\Delta$*  spinal cords (5  $\mu$ M, N = 7/9; 7  $\mu$ M and 10  $\mu$ M NMDA, N = 9/9) (Fig. 6A, lower traces). The locomotor frequency obtained in *ChAT-Vglut2 $\Delta/\Delta$*  cords was not significantly different from that of controls at any NMDA concentration tested ( $p > 0.3$ ) (controls:  $0.27 \pm 0.02$  Hz at 5  $\mu$ M,  $0.32 \pm 0.01$  Hz at 7  $\mu$ M,  $0.40 \pm 0.02$  Hz at 10  $\mu$ M; *ChAT-Vglut2 $\Delta/\Delta$*  cords:  $0.27 \pm 0.01$  Hz at 5  $\mu$ M;  $0.32 \pm 0.01$  Hz at 7  $\mu$ M,  $0.37 \pm 0.01$  Hz at 10  $\mu$ M) (Fig. 6B). Additionally, there was no significant difference in left-right (LL2-rL2) and flexor-extensor (rL2-rL5) phasing between control and *ChAT-Vglut2 $\Delta/\Delta$*  spinal cords (Watson-William's Test,  $p > 0.4$ ). Left-right and flexor-extensor activities were in alternation in both control and *ChAT-Vglut2 $\Delta/\Delta$*  cords. Mean left-right phase values (Fig. 6C, left) were 0.47 (5  $\mu$ M, N = 6) and 0.47 (7  $\mu$ M NMDA, N = 6) for controls, and 0.50 (5  $\mu$ M NMDA, N = 8) and 0.51 (7  $\mu$ M NMDA, N = 9) for *ChAT-Vglut2 $\Delta/\Delta$*  cords. Mean flexor-extensor phase values (Fig. 6C, right) were 0.51 (5  $\mu$ M, N = 4) and 0.43 (7  $\mu$ M NMDA, N = 4) for controls, and 0.51 (5  $\mu$ M NMDA, N = 8) and 0.47 (7  $\mu$ M NMDA, N = 9) for *ChAT-Vglut2 $\Delta/\Delta$*  cords.

To further verify if there were any deficits to the rhythm generating network due to the loss of glutamatergic transmission in motor neurons, we also used descending stimulation to evoke locomotion. Locomotor-like activity was evoked in all control (N = 6/6) and *ChAT-Vglut2 $\Delta/\Delta$*  (N = 9/9) spinal cords. In keeping with the results obtained from drug-induced locomotor studies, upon neural-evoked stimulation, no significant difference in locomotor frequency was observed between *ChAT-Vglut2 $\Delta/\Delta$*  and control cords at any of the stimulation intensities tested, 100  $\mu$ A – 1 mA ( $p > 0.3$ ) (Fig. 6D).

Collectively, these data indicate that the reduction in locomotor frequency we observe in *Hb9::Cre-Vglut2 $\Delta/\Delta$*  cords is due to the loss of glutamatergic synaptic transmission in *Hb9::Cre*-derived INs and not in motor neurons.

## Discussion

In this study, we have used the *Hb9::Cre* mouse line to identify *Hb9::Cre*-derived INs, target the excitatory subset of these neurons for removal from the spinal network, and investigate the consequences of their removal on motor output. Our findings provide insight into the involvement of these neurons in mammalian locomotor rhythm generation.

*Hb9::Cre* mice<sup>40</sup> were generated with an analogous strategy to the *Hb9-LacZ* mice<sup>31</sup>. However, a larger population of ventral as well as dorsal neurons is apparent in the *Hb9::Cre;Rosa26-FP* mouse. This is possibly due to the transient embryonic expression of *Hb9* in progenitor cells and postmitotic neurons<sup>32</sup> which is captured by the Cre-line. Here, we have collectively referred to the dorsal and ventral populations visualized in *Hb9::Cre;Rosa26-FP* mice as *Hb9::Cre*-derived INs.

Since in limbed animals the spinal locomotor networks are distributed rostral-caudally along the ventral lumbar spinal cord<sup>5,20</sup>, the fact that the *Hb9::Cre* mouse also includes cells in the dorsal spinal cord does not hinder its use as a tool to study the role of excitatory *Hb9::Cre*-derived INs in locomotion. Moreover, despite the large number and laminar distribution of *Hb9::Cre*-derived INs, they comprise a reliably identifiable population of interneurons. The same neurons are visualized by reporter expression in all *Rosa26* lines throughout the lumbar spinal cord. Additionally, as demonstrated by *Vglut2* mRNA *in situ*, this same visualized population is manipulated in the *Hb9::Cre-Vglut2 $\Delta/\Delta$*  mice.

Therefore, by using Cre-Lox recombination, we were able to reliably manipulate a group of excitatory INs which does not correspond to any of the known major excitatory ipsilaterally-projecting classes of neurons. In particular, excitatory *Hb9::Cre*-derived INs delineate a group of neurons that is distinct from the only other excitatory neuronal population that has been shown to play a role in mammalian locomotor rhythm generation, the *Shox2* non-V2a neurons<sup>28</sup>.

The cardinal feature that should characterize rhythm-generating neurons is that their selective manipulation should have a direct impact on locomotor frequency. Their activation should be able to initiate locomotor rhythm and/or change the frequency of the ongoing rhythm whereas a selective reduction in their number should reduce the frequency of the ongoing locomotor rhythm<sup>1,4,9,23,28,48,49</sup>. The most conclusive test to determine the effects of a given group of neurons on locomotor activity is achieved by an acute activation or inactivation of these neurons. However, the combination of channelrhodopsin (or other cell activator or inactivator) mouse lines with *Hb9::Cre* mice would lead to expression in both inhibitory and excitatory *Hb9::Cre*-derived INs as well as in MNs, thus confounding results. The inclusion of MNs in the population makes optogenetic or chemogenetic perturbation



experiments impossible to perform. Therefore, we instead pursued the functional removal of glutamatergic Hb9::Cre-derived INs from the network by selectively deleting *Vglut2* from the excitatory Hb9::Cre-derived population. By silencing the output of glutamatergic Hb9::Cre-derived INs and studying motor output in an isolated spinal cord preparation, we have shown that excitatory Hb9::Cre-derived INs are likely part of the locomotor rhythm generator, as demonstrated by the reduced locomotor frequency. In contrast, silencing the output of *Vglut2*-expressing Hb9::Cre-derived INs had no effect on patterning, including left-right and flexor-extensor alternations, unlike what has been described for the manipulation of excitatory V2a, V0 or V3 neurons<sup>12–14,16,50</sup>. We acknowledge, however, that distinguishing between a role in tonic drive to the rhythm generator and a role in rhythm generation per se is difficult and nearly impossible experimentally, and therefore, we cannot exclude that this decrease in frequency might be partly due to a reduction in tonic drive to the rhythm generating core.

The fact that some of the spinal cords from *Hb9::Cre-Vglut2 $\Delta/\Delta$*  mice did not respond to descending fiber stimulation may suggest that glutamatergic Hb9::Cre-derived INs play a role in mediating the initiation of locomotion. Thus, it is possible that the descending command system which initiates locomotion may target glutamatergic Hb9::Cre-derived INs and, due to the functional inactivation of these glutamatergic interneurons in *Hb9::Cre-Vglut2 $\Delta/\Delta$*  mice, locomotion is less readily evoked by stimulation of the descending fibers.

With the genetic tools at hand, it is not possible to determine whether the canonical Hb9 INs are partly or solely accountable for the locomotor phenotype we observe in *Hb9::Cre-Vglut2 $\Delta/\Delta$*  spinal cords. However, canonical Hb9 INs make up less than 1% of the Hb9::Cre-derived INs, and 33% of these Hb9::Cre-derived INs are excitatory. Therefore, the canonical Hb9 INs would be a negligible portion of the excitatory Hb9::Cre-derived INs (<3%). Accordingly, in *Hb9::Cre-Vglut2 $\Delta/\Delta$*  cords, the small number of canonical Hb9 neurons as compared to the total number of excitatory Hb9::Cre-derived INs, makes it less likely that the canonical Hb9 interneurons alone are responsible for the observed phenotype.

It should be emphasized that, similarly to what was concluded in studies on *Shox2* neurons<sup>28</sup>, we believe that it is unlikely that excitatory Hb9::Cre-derived INs are the sole rhythm-generating neurons in the mammalian locomotor network. In the absence of excitatory Hb9::Cre-derived INs, locomotor frequency is reduced but locomotor rhythm is not abolished. This is seen more clearly when compared to experiments where all excitatory neurons are silenced, which leads to a complete cessation of the rhythm<sup>23</sup>. These observations suggest that several molecularly distinct groups of neurons may contribute to rhythm generation. A distribution of rhythm generation between molecularly distinct groups of excitatory neurons is also seen in young zebrafish where excitatory commissural neurons<sup>51–53</sup> and V2a domains are involved in rhythm generation<sup>54–56</sup>. However, the corresponding *Shox2* INs and excitatory Hb9::Cre-derived INs have not yet been identified in the zebrafish.

Our classification of neurons as Hb9::Cre-derived INs does not sprout from the initial progenitor domain-defined classes of interneurons<sup>7</sup>. Instead, Hb9::Cre-derived INs, here, are those identified in the *Hb9::Cre* mouse line<sup>40</sup>. We have shown that excitatory Hb9::Cre-derived INs are a heterogeneous group of neurons that span several of the transcription factor-defined interneuron classes. Similarly, studies on *Shox2* INs have shown that even within *Shox2* non-V2a neurons, rhythm generation may be distributed amongst neurons derived from several progenitor domains<sup>28</sup>. Collectively, these data suggest that glutamatergic neurons spanning several classes of the known molecularly defined groups of neurons are responsible for rhythm generation. Therefore, it is plausible that, in the same way as new markers for acetylcholinergic spinal neurons<sup>57,58</sup> and inhibitory neurons<sup>59,60</sup> were identified, a comprehensive transcriptome screening to define a finer-grained molecular code of spinal glutamatergic neurons may define new markers for excitatory neurons that may help to clarify the identity of the functional subgroups involved in mammalian locomotor rhythm generation.

**Experimental Procedures.** *Mouse lines.* All experimental procedures followed the guidelines of the Animal Welfare Agency and were approved by the local ethical committee, Stockholms Norra Djurförsöksetisk nämnd. The following transgenic lines were used: *Hb9::Cre* (B6;129S-Mnx1tm4(cre)Tmj/J) mice obtained from the Jackson Laboratory see ref. 40; *Vglut2<sup>Flox/Flox</sup>* and *Vglut2 $\Delta/\Delta$*  mice kindly provided by Drs. T. Hnasko and R. Palminter<sup>61</sup>; *Vglut2-GFP* mice generated in our lab by Dr. Borgius using BAC recombination with an analogous strategy to the one described previously<sup>62</sup> (Supplementary Figure 1); *Hb9-GFP* (B6.Cg-Tg(Hlxb9-GFP)1Tmj/J) mice obtained from the Jackson Laboratory; *GlyT2-GFP* mice kindly provided by Dr. H.U. Zeilhofer<sup>63</sup>; *GAD67-GFP* mice provided by Dr. Y. Yanagawa<sup>64</sup>; *ChAT::Cre* (B6;129S6-Chattm2(cre)Lowl/J) mice, *Rosa26-YFP* (*Rosa26<sup>FloxedSTOP-YFP</sup>*) and *Rosa26-tdTomato* (*Rosa26<sup>FloxedSTOP-TdTomato</sup>*) mice obtained from the Jackson Laboratory.

For conditional deletion of *Vglut2*, *Vglut2<sup>Flox/Flox</sup>* mice with loxP sites flanking exon 2 of the *Slc17a6* gene, which encodes for *Vglut2*, were used (see ref. 17). To avoid germ-line recombination we first crossed either *Hb9::Cre* or *ChAT::Cre* with *Vglut2 $\Delta/\Delta$*  mice to obtain the double transgenic lines *Hb9::Cre;Vglut2 $\Delta/\Delta$*  or *ChAT::Cre;Vglut2 $\Delta/\Delta$* . These double transgenic lines were then crossed with the homozygous *Vglut2<sup>Flox/Flox</sup>*; *Rosa26-YFP* mice to generate *Hb9::Cre;Vglut2 $\Delta/\Delta$*  or *ChAT::Cre;Vglut2 $\Delta/\Delta$*  mice (see ref. 28), with conditional removal of *Vglut2* and conditional expression of YFP.

For neurotransmitter phenotyping *Vglut2-GFP*, *Gad67-GFP* or *Glyt2-GFP* mice were crossed with the reporter line *Rosa26-tdTomato* to obtain the double transgenic lines *Vglut2-GFP;Rosa26-tdTomato*, *Gad67-GFP;Rosa26-tdTomato* or *Glyt2-GFP;Rosa26-tdTomato*. These double transgenic lines were then crossed with *Hb9::Cre* mice to generate the triple transgenic lines *Hb9::Cre;Rosa26-tdTomato;Vglut2-GFP*, *Hb9::Cre;Rosa26-tdTomato;Gad67-GFP*, or *Hb9::Cre;Rosa26-tdTomato;Glyt2-GFP*.

*In Situ Hybridization, Immunohistochemistry and Cell Counts.* Spinal cords from embryonic mice at stage E11.5 and lumbar spinal cords from newborn mice at P0 were immersion fixed in 4% paraformaldehyde (2 hours at room temperature for immunohistochemistry or 24 hours at 4 °C for *in situ* hybridization), cryopreserved in 30% sucrose overnight, and stored at –80 °C. Serial transverse sections of embryonic spinal cords and newborn lumbar spinal cords were cryostat sectioned (20  $\mu$ m) and mounted on Menzel-Glaser SuperFrost slides. All slides

were stored at  $-80^{\circ}\text{C}$ . Sections were incubated for 24 hours with one or several of the following primary antibodies: rabbit anti-Shox2 #860 (1:32,000, generated against the peptide CKTTSKNSSIADLR), sheep anti-Chx10 (1:400, Chemicon), mouse anti-Isl1 (40.2D6 and 39.4D5) (1:250, DSHB), rabbit anti-Hb9 (1:16000, DSHB). The specificity of these antibodies has been evaluated and described in previous publications (see refs 12, 28 and 35). Secondary antibodies were obtained from Jackson ImmunoResearch or Invitrogen, used at 1:500 and incubated for 2 hours at room temperature.

Combined fluorescent *in situ* hybridization and immunofluorescence labeling was performed as previously described<sup>65</sup> using an antisense digoxigenin (DIG)-labeled RNA probe for vesicular glutamate transporter 2 (Vglut2) that spans base pairs 540 to 983 (produced by Dr. L. Borgius). Sections were blocked with 0.5% Blocking reagent (PerkinElmer) in TNT (0.1 M Tris-HCl pH7.5, 0.15 M NaCl, 0.1% (wg/vol) Tween20) and incubated with sheep anti-DIG peroxidase (1:2000, Roche Diagnostics). Signal was detected by tyramide-cyanine 3 (Cy3) amplification (1:50, PerkinElmer).

Slides were mounted in Vectashield reagent (Vector Laboratories), and images were scanned on a LSM510 Confocal Microscope (Zeiss Microsystems) using 10x and 20x objectives. Multiple channels were scanned sequentially to prevent fluorescence bleed through and false-positive signals. A contrast enhancement and noise reduction filter were applied in ImageJ for publication images.

Counts were done manually using a cell-counter plug-in in ImageJ, in 4–11 non-adjacent sections per mice ( $N = 2-4$ ) in each condition. Cellular counts per hemi-section were averaged per individual animal, and a grand-mean  $\pm$  standard error of the mean (SEM) was calculated across animals to produce percentage of cell per hemi-section bar-graphs.

**In Vitro Recording of Locomotor-Like Activity.** Spinal cords from newborn mice at P0 were dissected in ice-cold low  $\text{Ca}^{2+}$  Ringer's solution in mM; (111 NaCl, 3 KCl, 11 glucose, 25  $\text{NaHCO}_3$ , 3.7  $\text{MgSO}_4$ , 1.10  $\text{KH}_2\text{PO}_4$  and 0.25  $\text{CaCl}_2$ ) pH adjusted to 7.4 with 95%  $\text{O}_2$ /5%  $\text{CO}_2$ . All preparations were transferred to a recording chamber and perfused with normal Ringer's solution in mM; (111 NaCl, 3 KCl, 11 glucose, 25  $\text{NaHCO}_3$ , 1.3  $\text{MgSO}_4$ , 1.1  $\text{KH}_2\text{PO}_4$ , 2.5  $\text{CaCl}_2$ , pH 7.4, aerated with 95%  $\text{O}_2$ /5%  $\text{CO}_2$ ) at a flow rate of 4–5 ml/min. All recordings were performed at room temperature. Locomotor-like activity was either induced by bath application of N-methyl-D-aspartate (NMDA; 5–10  $\mu\text{M}$ ) and serotonin (5-HT; 5–8  $\mu\text{M}$ ) or evoked by electric stimulation of descending pathways<sup>66</sup>. Briefly, the electrical stimulation protocol entails a large suction electrode (approximately 100  $\mu\text{m}$  in tip diameter) used to deliver large amplitude (0.1–1 mA), long duration (10 ms) and low frequency (2 Hz) stimuli at the midline over the C1–C2 segments. The total duration of each train of stimuli was 60 seconds.

Recordings were obtained using glass suction electrodes attached to lumbar ventral roots (VRs) L2 or L5 on the left and right sides of the cord. VR signals were AC recorded and band-pass filtered from 100 to 1000 Hz (gain 5–10,000), digitized, and acquired with pCLAMP software (version 10; Molecular Devices).

**Locomotor analysis.** Locomotor frequency (Hz) (defined as the reciprocal of locomotor cycles) was calculated from 3–5 min of activity, taken at least 15 min after the initial burst of drug-induced activity, when locomotor-like activity had stabilized. Locomotor-like activity was analysed using rectified, smoothed (time constant of 0.2 s) and filtered AC signals of VR activity in Spike2 (Cambridge Electronic Design). Statistical significance was determined using two-way ANOVA and Sidak's multiple comparisons test or multiple T test using the Holm-Sidak method, with  $\alpha = 5.000\%$  ( $p < 0.05$ ). All p-values were adjusted to account for multiple comparisons. Data are expressed as mean  $\pm$  standard error of the mean (SEM).

For the analysis of left-right and flexor-extensor coordination, 50 random locomotor cycles were selected. Left (l) L2 VR was chosen as the reference trace while right (r) L2 and rL5 VRs were used as test traces. Circular statistics were used to determine the phase relationship between ipsilateral and contralateral VRs during locomotor-like rhythmic activity as previously described<sup>13,17,20</sup>.

The onset of a locomotor burst in the reference trace corresponds to the phase value of 0 in the circular plot and the onset of the next burst corresponds to a phase value of 1. For test traces, a phase value of 0.5 corresponds to alternation while a phase value of 1 (or 0) corresponds to synchrony. The mean timing of the 50 phase values was calculated as a vector in the circular plot where the resulting vector length ( $r$ ) reflects the concentration of phase values around the mean. Rayleigh's test<sup>67</sup> was used to determine whether  $r$  values reached statistical significance ( $p < 0.05$ ). Points falling inside the inner circle are not significant while those outside the inner circle are significant. Data are expressed as grand mean for each drug concentration. Watson-Williams test<sup>67</sup> was used to determine significant differences amongst conditions ( $p < 0.05$ ).

## References

1. Grillner, S. & Jessell, T. M. Measured motion: searching for simplicity in spinal locomotor networks. *Current opinion in neurobiology* **19**, 572–586, doi: 10.1016/j.conb.2009.10.011 (2009).
2. Kiehn, O. Locomotor circuits in the mammalian spinal cord. *Annual review of neuroscience* **29**, 279–306, doi: 10.1146/annurev.neuro.29.051605.112910 (2006).
3. Goulding, M. Circuits controlling vertebrate locomotion: moving in a new direction. *Nature reviews. Neuroscience* **10**, 507–518, doi: 10.1038/nrn2608 (2009).
4. Kiehn, O. Decoding the organization of spinal circuits that control locomotion. *Nature reviews. Neuroscience* **17**, 224–38, doi: 10.1038/nrn.2016.9 (2016).
5. Kiehn, O. & Kjaerulff, O. Distribution of central pattern generators for rhythmic motor outputs in the spinal cord of limbed vertebrates. *Annals of the New York Academy of Sciences* **860**, 110–129 (1998).
6. Goulding, M. & Pfaff, S. L. Development of circuits that generate simple rhythmic behaviors in vertebrates. *Current opinion in neurobiology* **15**, 14–20, doi: 10.1016/j.conb.2005.01.017 (2005).
7. Jessell, T. M. Neuronal specification in the spinal cord: inductive signals and transcriptional codes. *Nature reviews. Genetics* **1**, 20–29, doi: 10.1038/35049541 (2000).

8. Kiehn, O. Development and functional organization of spinal locomotor circuits. *Current opinion in neurobiology* **21**, 100–109, doi: 10.1016/j.conb.2010.09.004 (2011).
9. McLean, D. L. & Dougherty, K. J. Peeling back the layers of locomotor control in the spinal cord. *Current opinion in neurobiology* **33**, 63–70, doi: 10.1016/j.conb.2015.03.001 (2015).
10. Kiehn, O. Decoding the organization of spinal circuits that control locomotion. *Nature reviews. Neuroscience* **17**, 224–238, doi: 10.1038/nrn.2016.9 (2016).
11. Quinlan, K. A. & Kiehn, O. Segmental, synaptic actions of commissural interneurons in the mouse spinal cord. *The Journal of neuroscience: the official journal of the Society for Neuroscience* **27**, 6521–6530, doi: 10.1523/JNEUROSCI.1618-07.2007 (2007).
12. Crone, S. A. *et al.* Genetic ablation of V2a ipsilateral interneurons disrupts left-right locomotor coordination in mammalian spinal cord. *Neuron* **60**, 70–83, doi: 10.1016/j.neuron.2008.08.009 (2008).
13. Talpalar, A. E. *et al.* Dual-mode operation of neuronal networks involved in left-right alternation. *Nature* **500**, 85–88, doi: 10.1038/nature12286 (2013).
14. Crone, S. A., Zhong, G., Harris-Warrick, R. & Sharma, K. In mice lacking V2a interneurons, gait depends on speed of locomotion. *The Journal of neuroscience: the official journal of the Society for Neuroscience* **29**, 7098–7109, doi: 10.1523/JNEUROSCI.1206-09.2009 (2009).
15. Lanuza, G. M., Gosgnach, S., Pierani, A., Jessell, T. M. & Goulding, M. Genetic identification of spinal interneurons that coordinate left-right locomotor activity necessary for walking movements. *Neuron* **42**, 375–386 (2004).
16. Zhang, Y. *et al.* V3 spinal neurons establish a robust and balanced locomotor rhythm during walking. *Neuron* **60**, 84–96, doi: 10.1016/j.neuron.2008.09.027 (2008).
17. Talpalar, A. E. *et al.* Identification of minimal neuronal networks involved in flexor-extensor alternation in the mammalian spinal cord. *Neuron* **71**, 1071–1084, doi: 10.1016/j.neuron.2011.07.011 (2011).
18. Britz, O. *et al.* A genetically defined asymmetry underlies the inhibitory control of flexor-extensor locomotor movements. *eLife* **4**, doi: 10.7554/eLife.04718 (2015).
19. Zhang, J. *et al.* V1 and v2b interneurons secure the alternating flexor-extensor motor activity mice require for limbed locomotion. *Neuron* **82**, 138–150, doi: 10.1016/j.neuron.2014.02.013 (2014).
20. Kjaerulff, O. & Kiehn, O. Distribution of networks generating and coordinating locomotor activity in the neonatal rat spinal cord *in vitro*: a lesion study. *The Journal of neuroscience: the official journal of the Society for Neuroscience* **16**, 5777–5794 (1996).
21. Kiehn, O. *et al.* Excitatory components of the mammalian locomotor CPG. *Brain research reviews* **57**, 56–63, doi: 10.1016/j.brainresrev.2007.07.002 (2008).
22. Hagglund, M., Borgius, L., Dougherty, K. J. & Kiehn, O. Activation of groups of excitatory neurons in the mammalian spinal cord or hindbrain evokes locomotion. *Nature neuroscience* **13**, 246–252, doi: 10.1038/nn.2482 (2010).
23. Hagglund, M. *et al.* Optogenetic dissection reveals multiple rhythmic modules underlying locomotion. *Proceedings of the National Academy of Sciences of the United States of America* **110**, 11589–11594, doi: 10.1073/pnas.1304365110 (2013).
24. Jordan, L. M., Liu, J., Hedlund, P. B., Akay, T. & Pearson, K. G. Descending command systems for the initiation of locomotion in mammals. *Brain research reviews* **57**, 183–191, doi: 10.1016/j.brainresrev.2007.07.019 (2008).
25. Kiehn, O. *et al.* Probing spinal circuits controlling walking in mammals. *Biochemical and biophysical research communications* **396**, 11–18, doi: 10.1016/j.bbrc.2010.02.107 (2010).
26. Bui, T. V. *et al.* Circuits for grasping: spinal d13 interneurons mediate cutaneous control of motor behavior. *Neuron* **78**, 191–204, doi: 10.1016/j.neuron.2013.02.007 (2013).
27. Zhong, G. *et al.* Electrophysiological characterization of V2a interneurons and their locomotor-related activity in the neonatal mouse spinal cord. *The Journal of neuroscience: the official journal of the Society for Neuroscience* **30**, 170–182, doi: 10.1523/JNEUROSCI.4849-09.2010 (2010).
28. Dougherty, K. J. *et al.* Locomotor rhythm generation linked to the output of spinal shox2 excitatory interneurons. *Neuron* **80**, 920–933, doi: 10.1016/j.neuron.2013.08.015 (2013).
29. Al-Mosawie, A., Wilson, J. M. & Brownstone, R. M. Heterogeneity of V2-derived interneurons in the adult mouse spinal cord. *The European journal of neuroscience* **26**, 3003–3015, doi: 10.1111/j.1460-9568.2007.05907.x (2007).
30. Lundfald, L. *et al.* Phenotype of V2-derived interneurons and their relationship to the axon guidance molecule EphA4 in the developing mouse spinal cord. *The European journal of neuroscience* **26**, 2989–3002, doi: 10.1111/j.1460-9568.2007.05906.x (2007).
31. Arber, S. *et al.* Requirement for the homeobox gene Hb9 in the consolidation of motor neuron identity. *Neuron* **23**, 659–674 (1999).
32. Lee, S. K., Jurata, L. W., Funahashi, J., Ruiz, E. C. & Pfaff, S. L. Analysis of embryonic motoneuron gene regulation: derepression of general activators function in concert with enhancer factors. *Development* **131**, 3295–3306, doi: 10.1242/dev.01179 (2004).
33. Wilson, J. M. *et al.* Conditional rhythmicity of ventral spinal interneurons defined by expression of the Hb9 homeodomain protein. *The Journal of neuroscience: the official journal of the Society for Neuroscience* **25**, 5710–5719, doi: 10.1523/JNEUROSCI.0274-05.2005 (2005).
34. Wilson, J. M., Cowan, A. I. & Brownstone, R. M. Heterogeneous electrotonic coupling and synchronization of rhythmic bursting activity in mouse Hb9 interneurons. *Journal of neurophysiology* **98**, 2370–2381, doi: 10.1152/jn.00338.2007 (2007).
35. Hinckley, C. A., Hartley, R., Wu, L., Todd, A. & Ziskind-Conhaim, L. Locomotor-like rhythms in a genetically distinct cluster of interneurons in the mammalian spinal cord. *Journal of neurophysiology* **93**, 1439–1449, doi: 10.1152/jn.00647.2004 (2005).
36. Hinckley, C. A. & Ziskind-Conhaim, L. Electrical coupling between locomotor-related excitatory interneurons in the mammalian spinal cord. *The Journal of neuroscience: the official journal of the Society for Neuroscience* **26**, 8477–8483, doi: 10.1523/JNEUROSCI.0395-06.2006 (2006).
37. Brownstone, R. M. & Wilson, J. M. Strategies for delineating spinal locomotor rhythm-generating networks and the possible role of Hb9 interneurons in rhythmogenesis. *Brain research reviews* **57**, 64–76, doi: 10.1016/j.brainresrev.2007.06.025 (2008).
38. Hinckley, C. A., Wiesner, E. P., Mentis, G. Z., Titus, D. J. & Ziskind-Conhaim, L. Sensory modulation of locomotor-like membrane oscillations in Hb9-expressing interneurons. *Journal of neurophysiology* **103**, 3407–3423, doi: 10.1152/jn.00996.2009 (2010).
39. Ziskind-Conhaim, L., Mentis, G. Z., Wiesner, E. P. & Titus, D. J. Synaptic integration of rhythmic neurons in the locomotor circuitry: the case of Hb9 interneurons. *Annals of the New York Academy of Sciences* **1198**, 72–84, doi: 10.1111/j.1749-6632.2010.05533.x (2010).
40. Yang, X. *et al.* Patterning of muscle acetylcholine receptor gene expression in the absence of motor innervation. *Neuron* **30**, 399–410 (2001).
41. Wichterle, H., Lieberam, I., Porter, J. A. & Jessell, T. M. Directed differentiation of embryonic stem cells into motor neurons. *Cell* **110**, 385–397 (2002).
42. Hess, D. M. *et al.* Localization of TrkC to Schwann cells and effects of neurotrophin-3 signaling at neuromuscular synapses. *The Journal of comparative neurology* **501**, 465–482, doi: 10.1002/cne.21163 (2007).
43. Liem, K. F., Jr., Tremml, G. & Jessell, T. M. A role for the roof plate and its resident TGFbeta-related proteins in neuronal patterning in the dorsal spinal cord. *Cell* **91**, 127–138 (1997).
44. Helms, A. W. & Johnson, J. E. Specification of dorsal spinal cord interneurons. *Current opinion in neurobiology* **13**, 42–49 (2003).
45. Nishimaru, H., Restrepo, C. E., Ryge, J., Yanagawa, Y. & Kiehn, O. Mammalian motor neurons corelease glutamate and acetylcholine at central synapses. *Proceedings of the National Academy of Sciences of the United States of America* **102**, 5245–5249, doi: 10.1073/pnas.0501331102 (2005).

46. Mentis, G. Z. *et al.* Noncholinergic excitatory actions of motoneurons in the neonatal mammalian spinal cord. *Proceedings of the National Academy of Sciences of the United States of America* **102**, 7344–7349, doi: 10.1073/pnas.0502788102 (2005).
47. Pujala, A., Blivis, D. & O'Donovan, M. J. Interactions between Dorsal and Ventral Root Stimulation on the Generation of Locomotor-Like Activity in the Neonatal Mouse Spinal Cord. *eNeuro* **3**, doi: 10.1523/ENEURO.0101-16.2016 (2016).
48. Roberts, A., Li, W. C. & Soffe, S. R. How neurons generate behavior in a hatchling amphibian tadpole: an outline. *Frontiers in behavioral neuroscience* **4**, 16, doi: 10.3389/fnbeh.2010.00016 (2010).
49. El Manira, A. Dynamics and plasticity of spinal locomotor circuits. *Current opinion in neurobiology* **29**, 133–141, doi: 10.1016/j.conb.2014.06.016 (2014).
50. Zhong, G., Sharma, K. & Harris-Warrick, R. M. Frequency-dependent recruitment of V2a interneurons during fictive locomotion in the mouse spinal cord. *Nature communications* **2**, 274, doi: 10.1038/ncomms1276 (2011).
51. McLean, D. L., Masino, M. A., Koh, I. Y., Lindquist, W. B. & Fetcho, J. R. Continuous shifts in the active set of spinal interneurons during changes in locomotor speed. *Nature neuroscience* **11**, 1419–1429, doi: 10.1038/nn.2225 (2008).
52. Fetcho, J. R. & McLean, D. L. Some principles of organization of spinal neurons underlying locomotion in zebrafish and their implications. *Ann Ny Acad Sci* **1198**, 94–104, doi: 10.1111/j.1749-6632.2010.05539.x (2010).
53. McLean, D. L. & Fetcho, J. R. Spinal Interneurons Differentiate Sequentially from Those Driving the Fastest Swimming Movements in Larval Zebrafish to Those Driving the Slowest Ones. *Journal of Neuroscience* **29**, 13566–13577, doi: 10.1523/Jneurosci.3277-09.2009 (2009).
54. McLean, D. L. & Fetcho, J. R. Using imaging and genetics in zebrafish to study developing spinal circuits *in vivo*. *Developmental neurobiology* **68**, 817–834, doi: 10.1002/dneu.20617 (2008).
55. Eklof-Ljunggren, E. *et al.* Origin of excitation underlying locomotion in the spinal circuit of zebrafish. *Proceedings of the National Academy of Sciences of the United States of America* **109**, 5511–5516, doi: 10.1073/pnas.1115377109 (2012).
56. Ljunggren, E. E., Haupt, S., Ausborn, J., Ampatzis, K. & El Manira, A. Optogenetic activation of excitatory premotor interneurons is sufficient to generate coordinated locomotor activity in larval zebrafish. *The Journal of neuroscience: the official journal of the Society for Neuroscience* **34**, 134–139, doi: 10.1523/JNEUROSCI.4087-13.2014 (2014).
57. Enjin, A. *et al.* Identification of novel spinal cholinergic genetic subtypes disclose Chodl and Ptx2 as markers for fast motor neurons and partition cells. *The Journal of comparative neurology* **518**, 2284–2304, doi: 10.1002/cne.22332 (2010).
58. Zagoraïou, L. *et al.* A cluster of cholinergic premotor interneurons modulates mouse locomotor activity. *Neuron* **64**, 645–662, doi: 10.1016/j.neuron.2009.10.017 (2009).
59. Bikoff, J. B. *et al.* Spinal Inhibitory Interneuron Diversity Delineates Variant Motor Microcircuits. *Cell*, doi: 10.1016/j.cell.2016.01.027 (2016).
60. Perry, S. *et al.* Firing properties of Renshaw cells defined by ChRNA2 are modulated by hyperpolarizing and small conductance ion currents Ih and ISK. *The European journal of neuroscience* **41**, 889–900, doi: 10.1111/ejn.12852 (2015).
61. Hnasko, T. S. *et al.* Vesicular glutamate transport promotes dopamine storage and glutamate corelease *in vivo*. *Neuron* **65**, 643–656, doi: 10.1016/j.neuron.2010.02.012 (2010).
62. Borgius, L., Restrepo, C. E., Leao, R. N., Saleh, N. & Kiehn, O. A transgenic mouse line for molecular genetic analysis of excitatory glutamatergic neurons. *Molecular and cellular neurosciences* **45**, 245–257, doi: 10.1016/j.mcn.2010.06.016 (2010).
63. Zeilhofer, H. U. *et al.* Glycinergic neurons expressing enhanced green fluorescent protein in bacterial artificial chromosome transgenic mice. *The Journal of comparative neurology* **482**, 123–141, doi: 10.1002/cne.20349 (2005).
64. Tamamaki, N. *et al.* Green fluorescent protein expression and colocalization with calretinin, parvalbumin, and somatostatin in the GAD67-GFP knock-in mouse. *The Journal of comparative neurology* **467**, 60–79, doi: 10.1002/cne.10905 (2003).
65. Borgius, L. *et al.* Spinal Glutamatergic Neurons Defined by EphA4 Signaling Are Essential Components of Normal Locomotor Circuits. *The Journal of neuroscience: the official journal of the Society for Neuroscience* **34**, 3841–3853, doi: 10.1523/JNEUROSCI.4992-13.2014 (2014).
66. Talpalar, A. E. & Kiehn, O. Glutamatergic mechanisms for speed control and network operation in the rodent locomotor CpG. *Frontiers in neural circuits* **4**, doi: 10.3389/fncir.2010.00019 (2010).
67. Zar, J. H. *Biostatistical analysis*. (Prentice-Hall, 1974).

## Acknowledgements

We are grateful to Dr. Thomas Hnasko for providing the *Vglut2<sup>Flox/Flox</sup>* and *Vglut2<sup>Δ/+</sup>* mice, Dr. Eva Hedlund and Dr. Ilary Allodi for providing the *Hb9-GFP* mice, Dr. Adolfo Talpalar for comments on a version of the manuscript, and to Ann-Charlotte Westerdahl, Anna Kasagiannis, and Natalie Sleiers for technical assistance. This work was supported by the Swedish Research Council (OK), ERC advanced grants NeuronsInMotion and LocomotorIntegration (OK), and StratNeuro (OK).

## Author Contributions

K.J.D. and O.K. conceived the electrophysiological study. V.C., K.J.D. and O.K. conceived the immunohistochemical study. V.C. and K.J.D. performed immunohistochemical investigations, *in vitro* recordings and analyzed data. L.B. generated the *Vglut2-GFP* mouse. V.C. and O.K. wrote the paper with contributions from all authors. O.K. supervised all aspects of the work.

## Additional Information

**Supplementary information** accompanies this paper at <http://www.nature.com/srep>

**Competing financial interests:** The authors declare no competing financial interests.

**How to cite this article:** Caldeira, V. *et al.* Spinal Hb9::Cre-derived excitatory interneurons contribute to rhythm generation in the mouse. *Sci. Rep.* **7**, 41369; doi: 10.1038/srep41369 (2017).

**Publisher's note:** Springer Nature remains neutral with regard to jurisdictional claims in published maps and institutional affiliations.



This work is licensed under a Creative Commons Attribution 4.0 International License. The images or other third party material in this article are included in the article's Creative Commons license, unless indicated otherwise in the credit line; if the material is not included under the Creative Commons license, users will need to obtain permission from the license holder to reproduce the material. To view a copy of this license, visit <http://creativecommons.org/licenses/by/4.0/>

© The Author(s) 2017